ELSEVIER

Thermochimica Acta 381 (2002) 45–48

thermochimica acta

www.elsevier.com/locate/tca

Thermal analysis on nanosized TiO_2 prepared by hydrolysis

Huaqing Xie*, Qinghong Zhang, Tonggeng Xi, Jinchang Wang, Yan Liu

Research and Development Center for Special Inorganic Materials, Shanghai Institute of Ceramics,
Chinese Academy of Sciences, 1295 Dingxi Road, Shanghai 200050, China

Received 18 January 2001; accepted 12 June 2001

Abstract

Nanosized titanium oxide (TiO_2) powders of various amorphous–anatase–rutile phases were prepared by hydrolysis using an economic inorganic compound $TiCl_4$ as precursor. The powders were characterized by transmission electron mocroscopy (TEM), X-ray diffraction (XRD) and Brunnauer-Emmett-Teller (BET) techniques. Thermogravimetry analysis (TGA), differential thermal analysis (DTA) and DSC were performed on the prepared powders. The effects of small amount of sulphate ions and hydrolysis temperature on the morphology and crystallization were analyzed. The mass fraction of nanosized amorphous TiO_2 was determined by DSC first time. © 2002 Elsevier Science B.V. All rights reserved.

Keywords: Nanosized TiO_2; Phase transformation; Thermal analysis

1. Introduction

Titania oxide (TiO_2) is a material used widely in the electronics, ceramics, catalysis, and pigment industries. In recent years, nanosized TiO_2 have been prepared and its physical and chemical properties are extensively studied to improve its activity because nanosized material has small primary particle size and enhancing specific surface area [1–3]. It is well known that amorphous, anatase and rutile are most common polymorphs of TiO_2. Most researchers believe that the morphology is the most primitive and essential properties of TiO_2 powders, e.g. anatase, but not rutile, crystallites have relatively high photocatalytic activity [4–6]. A good understanding of the morphology and crystallization of nanosized TiO_2 powders prepared by different techniques and processed under different conditions is helpful to control the processes on nucleation, grain growth, and the phase transformation of nanosized TiO_2, and thus, is fundamental to their applications. Normally, the fraction of anatase and rutile in a sample is determined via the usually accepted quantitative method [7,8]. This method consists of measuring the relative X-ray diffraction (XRD) intensities of the anatase [1 0 1] and rutile [1 1 0]. However, to the best of our knowledge, there is no literature available on how to determine the fraction of nanosized amorphous TiO_2 directly.

In the present work, nanosized TiO_2 powders were prepared by the hydrolysis of $TiCl_4$ in aqueous solution. In order to investigate the effects of the temperature of hydrolysis and sulphate ions on the morphology and characterization, samples containing various amorphous–anatase–rutile phases were prepared and thermal analysis associated with transmission electron mocroscopy (TEM), XRD and Brunnauer-Emmett-Teller (BET) techniques were performed on the as-prepared samples.

---

* Corresponding author. Tel.: +86-21-625-12990;
fax: +86-21-625-13903.
E-mail address: huaqing_xie@hotmail.com (H. Xie).

PII: S0040-6031(01)00642-6

2. Experimental

2.1. Sample preparation

Nanosized TiO_2 powders were prepared by controlling the hydrolysis of $TiCl_4$ in aqueous solution. The detailed procedure is described in [9]. To investigate the effects of the temperature of hydrolysis and sulphate ions on the crystalline morphology, the hydrolysis temperature were varied in the 20–95 °C range and the aqueous solutions containing precursors were mixed with distilled water or $(NH_4)_2SO_4$ solution. The preparing conditions of the samples are summarized in Table 1 (samples #1 to #5). In order to determine the crystallization enthalpy of amorphous TiO_2, The prepared nanosized amorphous TiO_2 power is mixed with anatase with particle size of 10 nm in desired weight fraction for drawing a calibration line.

2.2. Characterization

The crystalline phases (anatase or rutile) of the as-prepared samples were determined by XRD patterns obtained on an automated diffractometer RAX-10. The specific surface area of the nanosized powder is measured by BET using a micromeritics ASAP 2010 nitrogen adsorption apparatus. The morphologies of the samples were observed by TEM (Jeol JEM2010 ultra high resolution TEM operating at 200 kV). The particle size was calculated using Scherrer formula and obtained by TEM observation.

2.3. Thermal analysis

To study the effect of the hydrolysis conditions on the crystalline morphology and the phase transformation of nanosized TiO_2, The samples were performed differential thermal analysis (DTA) by a SHIMADZU DTA-50H. The fraction of the absorption water or organic of the samples is determined by thermogravimetry analysis (TGA) using a SHIMADZU TGA-50H. The crystalline phase transformation temperature and enthalpy were measured by using a differential scanning calorimeter (SHIMADZU DSC-50). From the enthalpy the fraction of amorphous phase is calculated. The heating rate of all the thermal analysis experiments is 10 °C min^{-1} and nitrogen with flux of 20 ml min^{-1} is applied for protective gas.

Table 1
The hydrolysis conditions of the as-used samples

	#1	#2	#3	#4	#5
Hydrolysis temperature (°C)	20	20	70	70	95
$[Ti]/[SO_4^{2-}]$	1:0	20:1	1:0	20:1	1:2

3. Results and discussion

The properties of the as-prepared samples are summarized in Table 2. XRD patterns show that samples #1 and #2 contain dominantly amorphous TiO_2, with a very small fraction of or without crystalline phase. Sample #1 has a specific surface area of 501 $m^2\ g^{-1}$ measured by BET techniques, slightly larger than that of sample #2. Regarding crystalline phase, sample #4 contains only anatase crystallite while sample #3 is a mixture of anatase and rutile. The results indicate that the addition of sulphate ions is quite effective in retarding the formation of rutile phase when $TiCl_4$ hydrolyzed at 70 °C. Sample #5 contains only anatase phase with the particle dimension of 3.8 nm.

Fig. 1 shows the particle surface area dependence of the weight loss of the samples. From the figure, the weight loss increase with the particle surface area, which means that TiO_2 with larger specific surface area absorbs more water or organic residue than that with smaller surface area. Because a key requirement to improve the activity of TiO_2 as catalyst is to enhance the gas absorbed, the samples (#1 and #2) with relatively larger surface area are potential to be used as catalyst supports.

The DTA results of the as prepared samples are shown in Fig. 2. Curves 1–5 are the DTA results of samples #1 to #5, respectively. On all the five curves, the endothermal peak around 70 °C and the exothermal peak around 280 °C are due to losing the water absorbed at the surface of particle and organic residue, respectively. The exothermal peak in the range of 400–480 °C is attributed to amorphous to anatase transformation and the peak in the range of 680–740 °C is due to anatase to rutile transformation, which the XRD results also indicate. By being heated, the phase transformation procedure is

$$\text{amorphous} \xrightarrow{400-480^{\circ}\mathrm{C}} \text{anatase} \xrightarrow{680-740^{\circ}\mathrm{C}} \text{rutile}$$

Table 2
The properties of the samples characterized by XRD, TEM and BET techniques

	#1	#2	#3	#4	#5
Particle size (nm) (calculated by XRD)	Amorphous	Amorphous	5.9 (A), 4.3 (R)	3.5 (A)	3.8 (A)
Surface area ($m^2 g^{-1}$) (BET)	501	470	271	383	290

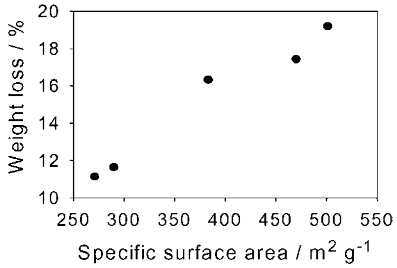

Fig. 1. Specific surface area dependence of the weight loss.

All curves 1–4 have exothermal peaks around 400–480 °C, with the area of the peak of curve 1 slightly larger than that of curve 2 and the area of the peak of curve 3 larger than that of curve 4. It means that all #1 to #4 samples contain amorphous TiO_2, with amorphous TiO_2 in sample #1 more than that in sample #2 and amorphous TiO_2 in sample #3 more than sample #4. Curve 5 indicates that there is no amorphous TiO_2 in sample #5. The exothermal peak around 680–740 °C of curve 2 is broader than that of curve 1 and this peak of curve 4 is broader than that of curve 3, which indicates that anatase–rutile transformation of sample #2 is slower than that of sample #2 and this transformation of sample #4 is slower than that of sample #3. The results are consistent with the XRD patterns. We ascribe the anatase–rutile transformation peak broadening to inhibition effect of trace sulphate ions.

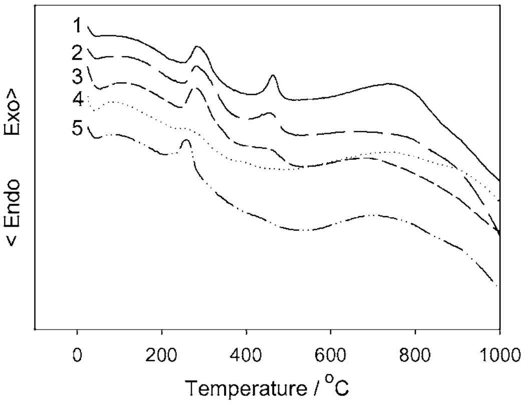

Fig. 2. DTA patterns of as-prepared samples.

The content of amorphous TiO_2 in a sample can be evaluated from the ratio of crystallization enthalpy between the values of the sample and pure amorphous TiO_2. A calibration line was drawn with the mixture of nanosized amorphous TiO_2 (sample #1) and anatase TiO_2 with an average diameter of 10 nm to determined the enthalpy of crystallization of amorphous TiO_2. The fraction of the added anatase TiO_2 was calculated by an equation of

$$f = \frac{w_2}{0.808w_1 + w_2} \quad (1)$$

where f is the fraction of added anatase TiO_2, w_1 the weight of sample #1, w_2 the weight of added anatase TiO_2. The calibration line is shown in Fig. 3. Least squares fitting of the experimental results gives an equation of

$$h = 217.8 - 233.3f \quad (2)$$

where h is the crystallization enthalpy of the mixture per gram. However, with a linear relation between

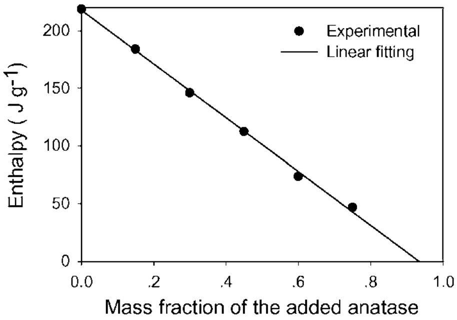

Fig. 3. A calibration line for crystalliztion enthalpy.

Table 3
The content of as-prepared samples

	#1	#2	#3	#4	#5
f_{abs}	0.192	0.174	0.111	0.163	0.116
f_{amor}	0.808	0.767	0.028	0.005	0
f_{ana}	0	0.059	0.315	0.832	0.884
f_{rut}	0	0	0.546	0	0

peak area and the fraction of amorphous TiO_2, f should be 1 where h is zero. The discrepancy might be caused by the marked difference in the specific surface area of the added anatase and the amorphous samples. From Eq. (2), the crystallization enthalpy of pure amorphous (h_0) was determined to be 217.8 J g^{-1}. The value was used as a standard to determine the weight fraction of amorphous (f_{amor}) by an equation

$$f_{amor} = \frac{H}{h_0 m_s} \tag{3}$$

where H is the peak area, m_s the sample weight.

The fraction of anatase and rutile is calculated via the relative XRD intensities of the anatase [1 0 1] ($d = 3.520$) and rutile [1 1 0] ($d = 3.247$) from the following equations

$$f_{rut} = \frac{(1 - f_{abs} - f_{amor})}{1 + 0.8\,(I_{ana}/I_{rut})} \tag{4}$$

and

$$f_{ana} = 1 - f_{abs} - f_{amor} - f_{rut} \tag{5}$$

where f is the mass fraction, I the X-ray integrated intensity, subscripts abs, amor, ana and rut represent water and organic residue, amorphous, anatase and rutile, repectively.

The fractions of water and organic residue (f_{abs}), amorphous (f_{amor}), anatase (f_{ana}) and rutile (f_{rut}) of samples #1 to #5 are summarized in Table 3. Comparing samples #1 to #2 and #3 to #4, it is quantitatively shown that, under the same hydrolysis temperature, the addition of a small amount of SO_4^{2-} promotes the formation of anatase phase. The mechanism may be that SO_4^{2-} ions induce the growth of TiO_2 clusters to anatase phase.

4. Conclusions

With controlling the hydrolysis conditions, either nanosized crystalline TiO_2 or amorphous TiO_2 with very large specific surface area were prepared by using an economic inorganic material $TiCl_4$ as precursor. The smallest particle size calculated by XRD pattern is 3.5 nm for anatase and the largest specific surface area measured by BET is 501 $m^2\,g^{-1}$. The water and organic residue absorbed by the particle surface increase with the specific surface area. The crystallization enthalpy of amorphous TiO_2 is 217.8 J g^{-1}. Thermal analysis coupled with XRD patterns revealed that the addition of a small amount of SO_4^{2-} promotes the formation of anatase phase and inhabits the anatase–rutile transformation.

Acknowledgements

The authors thank Natural Science Foundation of China (no. 50006014) for financial support.

References

[1] J.Y. Chen, L. Gao, J.H. Huang, J. Mater. Sci. 31 (1996) 3497.

[2] D.C. Hague, M.J. Mayo, J. Am. Ceram. Soc. 77 (1994) 1957.

[3] K.P. Kumar, K. Keizer, K. Bruggraaf, Nature 358 (1992) 48.

[4] B. Ohtani, Y. Ogawa, S. Nishimoto, J. Phys. Chem. B 101 (1997) 3746.

[5] B. Kraeutler, A.J. Bard, J. Am. Chem. Soc. 100 (1978) 5985.

[6] M.V. Rao, K. Rajeswar, V.R. Pai, J. Dubow, J. Phys. Chem. 84 (1980) 1987.

[7] A.A. Gribb, J.F. Banfield, Am. Min. 82 (1997) 717.

[8] H. Zhang, J.F. Banfield, J. Mater. Res. 15 (2000) 437.

[9] O. Zhang, L. Gao, J. Guo, J. Eur. Ceram. Soc. 20 (2000) 2153.